


RESEARCH

Open Access



Lipid reprogramming induced by the TFEB-ERR α axis enhanced membrane fluidity to promote EC progression

Xiaodan Mao^{1,2,3,4†}, Huifang Lei^{1†}, Tianjin Yi⁵, Pingping Su¹, Shuting Tang¹, Yao Tong¹, Binhua Dong^{1,3}, Guanyu Ruan^{1,3}, Alexander Mustea⁶, Jalid Sehouli⁷ and Pengming Sun^{1,3,4*} 

Abstract

Background: Estrogen-related receptor α (ERR α) has been reported to play a critical role in endometrial cancer (EC) progression. However, the underlying mechanism of ERR α -mediated lipid reprogramming in EC remains elusive. The transcription factor EB (TFEB)-ERR α axis induces lipid reprogramming to promote progression of EC was explored in this study.

Methods: TFEB and ERR α were analyzed and validated by RNA-sequencing data from the Cancer Genome Atlas (TCGA). The TFEB-ERR α axis was assessed by dual-luciferase reporter and chromatin immunoprecipitation quantitative polymerase chain reaction (ChIP-qPCR). The mechanism was investigated using loss-of-function and gain-of-function assays in vitro. Lipidomics and proteomics were performed to identify the TFEB-ERR α -related lipid metabolism pathway. Pseudopods were observed by scanning electron microscope. Furthermore, immunohistochemistry and lipidomics were performed in clinical tissue samples to validate the ERR α -related lipids.

Results: TFEB and ERR α were highly expressed in EC patients and correlated to EC progression. ERR α is the direct target of TFEB to mediate EC lipid metabolism. TFEB-ERR α axis mainly affected glycerophospholipids (GPs) and significantly elevated the ratio of phosphatidylcholine (PC)/sphingomyelin (SM), which indicated the enhanced membrane fluidity. TFEB-ERR α axis induced the mitochondria specific phosphatidylglycerol (PG) (18:1/22:6) + H increasing. The lipid reprogramming was mainly related to mitochondrial function though combining lipidomics and proteomics. The maximum oxygen consumption rate (OCR), ATP and lipid-related genes *acc*, *fasn*, and *acadm* were found to be positively correlated with TFEB/ERR α . TFEB-ERR α axis enhanced generation of pseudopodia to increase the invasiveness. Mechanistically, our functional assays indicated that TFEB promoted EC cell migration in an ERR α -dependent manner via EMT signaling. Consistent with the in vitro, higher PC (18:1/18:2) + HCOO was found in EC patients, and those with higher TFEB/ERR α had deeper myometrial invasion and lower serum HDL levels. Importantly, PC (18:1/18:2) + HCOO was an independent risk factor positively related to ERR α for lymph node metastasis.

Conclusion: Lipid reprogramming induced by the TFEB-ERR α axis increases unsaturated fatty acid (UFA)-containing PCs, PG, PC/SM and pseudopodia, which enhance membrane fluidity via EMT signaling to promote EC progression.

*Correspondence: sunfemy@hotmail.com

[†]Xiaodan Mao and Huifang Lei contributed equally to this work.

¹ Laboratory of Gynecologic Oncology, Department of Gynecology, Fujian Maternity and Child Health Hospital, Affiliated Hospital of Fujian Medical University, No. 18 Daoshan Road, Fuzhou 350001, China
Full list of author information is available at the end of the article



PG (18:1/22:6) + H induced by TFEB-ERR α axis was involved in tumorigenesis and PC (18:1/18:2) + HCOO was the ERR α -dependent lipid to mediate EC metastasis.

Keywords: TFEB, ERR α , Endometrial cancer, Lipid reprogramming, Mitochondrial stress, EMT signaling

Background

High body mass index (BMI) influences the current and future health of patients and is considered one of the top 5 global causes of death for females [1]. Among all female malignancies, endometrial cancer (EC) is most strongly associated with obesity, and obesity has been considered a very important risk factor for EC in postmenopausal women [2]. EC is the sixth most common cancer in women and the second most common gynecological malignancy globally. There were approximately 66,570 new cases and 12,940 reported deaths due to EC in the United States in 2021 [3]. The incidence of EC has also markedly increased in China recently. The age-standardized incidence of EC was 63.4 per 100,000, the mortality rate was 21.8 per 100,000, and the 5-year relative survival was 72.8% from 2012–2015 [4]. Considering the accompanying symptoms of overweight and diabetes in EC patients, tumor lipid metabolism has been the research focus. However, the mechanism of lipid metabolism in EC is still unclear.

Estrogen-related receptor α (ERR α , NR3B1, ESRRA) is a constitutively active ligand-independent orphan nuclear receptor that belongs to the nuclear receptor superfamily [5]. As a transcription factor, ERR α combines with its acknowledged coactivator peroxisome proliferator-activated receptor (PPAR) coactivator-1 α (PGC-1 α) and plays a central role in the regulation of cellular oxidative phosphorylation and liposome metabolism, resulting in many biological functions [6, 7]. Consistent with an increasing number of studies on breast cancer [8], colon cancer [9] and ovarian cancer [10], our previous works confirmed that high expression of ERR α was significantly related to a poor prognosis in EC [10]. Moreover, overexpression of ERR α can downregulate the expression of E-cadherin while upregulating the expression of vimentin and inducing epithelial-mesenchymal transformation (EMT), which promotes invasion and migration, indicating that it may be a new biomarker for predicting the risk of deep myometrial invasion and metastasis [11]. After targeted inhibition of ERR α by small interfering RNA (siRNA) or antagonist XCT790, transcription factor EB (TFEB) was identified as a potential interacting protein by a DNA/protein high-throughput assay [12]. TFEB, a master regulator of lysosomal biogenesis and autophagy, was found to have a crucial pathogenic role in different tumors [13]. Several recent studies have also focused on the function of TFEB in tumor cell metabolism. Carmine

et al. suggested that TFEB might be a novel therapeutic target for disorders of lipid metabolism, such as fatty liver disease, and that TFEB exerts global transcriptional control on lipid catabolism via PGC-1 α and PPAR α [14]. However, there were only very few reports about the association between TFEB and ERR α aside from those published by our team.

The EMT program is related to lipid remodeling of the cell membrane [15]. The fatty acyl moieties of membrane phospholipids exhibit considerable diversity in chain length and different degrees of saturation, which determine the biophysical properties of membranes, including their fluidity, curvature, and subdomain architecture [16]. The major structural phospholipids in mammalian membranes are glycerophospholipids (GPs), among which phosphatidylcholine (PC) is the most abundant in mammalian cell membranes and subcellular organelles, accounting for 40–50% of total phospholipids [17]. The saturability of PC affects the plasma membrane of tumor cells to sustain oncogenic activity in a wide variety of cancers [16, 18]. Lin et al. showed that the length of the fatty acid chain in the membrane modulated plasma membrane fluidity and invasion of liver cancer [19]. The roles of lipid metabolism in the function of the membrane in EC still need to be unveiled. Interestingly, both ERR α and TFEB were reported to be involved in the lipid remodeling signaling pathway.

How ERR α and TFEB play roles in lipid metabolism and how this mechanism affects malignant cell metastasis and invasion still need more research. We hypothesized that TFEB-ERR α signaling, which regulates lipid metabolism, extensively affects membrane function to promote EC invasion and metastasis. In this work, our discovery discusses the crosstalk between TFEB and ERR α and their coregulation of FA metabolism to promote invasion and metastasis in EC.

Materials and methods

Cell lines and cell culture

Human KLE endometrial adenocarcinoma cells were obtained from the Shanghai Cell Biological Research Institute (Shanghai, China), and ECC-1 cells were acquired from the American Type Culture Collection (ATCC, USA). KLE cells are ER α -, while ECC-1 cells are ER α +. KLE and ECC-1 cells were thawed and cultured in DMEM/F12 medium (#A4192001, Thermo Fisher, Waltham, MA, USA), 1% antibiotic-antimycotic

solution (#B120901, BasalMedia, Shanghai, China), and 10% fetal bovine serum (FBS) (#2275129, Gibco, Inchinnan, UK) at 37 °C in 5% CO₂. Cells treated with XCT790 (#725247-18-7, Sigma-Aldrich, St. Louis, MO, USA) were incubated in phenol red-free medium (#21041025, Thermo Fisher, Waltham, MA, USA) containing 1% serum replacement 1 (#S0638, Sigma-Aldrich, St. Louis, MO, USA). ECC-1 and KLE were incubated with 10 μM XCT790 (in dimethyl sulfoxide [DMSO]; #Y190601, MP Biomedicals LLC, Santa Ana, CA, USA) or DMSO (control) for 24 h. Lentiviral vectors expressing siRNAs targeting TFEB (named TFEB-KD) and ERRα (named ERRα-KD) were constructed. The following siRNA target sequence in the TFEB gene (GenBank accession No. NM_001167827.3) was selected: 5'-GAG ACG AAG GTT CAA CAT CAA-3'. The siRNA target sequence in the ERRα (GenBank accession NM_004451.5) was 5'-GAG CGA GAG TAT GTT CTA-3'. The lentiviral vector used to overexpress TFEB and ERRα were named TFEB-OV and ERRα-OV, respectively. Overexpression of ERRα or TFEB was achieved in KLE and ECC-1 cells and named KLE^{TFEB-OV}, ECC-1^{TFEB-OV}, KLE^{ERRα-OV} and ECC-1^{ERRα-OV}, respectively. In addition, KLE and ECC-1 cells with ERRα or TFEB expression downregulated through lentivirus-mediated siRNA were named KLE^{TFEB-KD}, ECC-1^{TFEB-KD}, KLE^{ERRα-KD} and ECC-1^{ERRα-KD}, respectively.

Bioinformatics data analyze

The Cancer Genome Atlas (TCGA) data of Uterine Corpus Endometrial Carcinoma (UCEC) were downloaded from Genomic Data Commons data portal <https://portal.gdc.cancer.gov/>. The dataset included 23 normal endometrial specimens and 543 EC specimens, with 9 repeated cancerous specimens excluded. Patient clinical information, gene-level copy number variation (CNV) profiles, gistic2 thresholds analyzed by the GISTIC2.0 method and somatic nonsilent mutation (gene-level) data were acquired from the University of California, Santa Cruz (UCSC) Xena website. The Database for Annotation, Visualization and Integrated Discovery (DAVID) (version 6.8) provides a comprehensive set of functional annotation tools that help investigators understand the biological meaning behind a large list of genes. GO functional annotation and KEGG analysis of the proteins were performed, and the results were visualized with the cluster Profiler R package (version 1.3.1093).

RNA extraction, RT-qPCR, Western blotting (WB)

Samples were collected from an equal number of intact cells in TRI Reagent® (#TR118; Molecular Research Center, Cincinnati, OH, USA). After reverse transcription on 500 ng of total RNA with GoScript™ Reverse

Transcription Mix, Oligo (dT) (#A2791, Promega, Madison, Wis, USA), quantitative PCR amplification was performed on the LightCycler 480 (Roche, Switzerland) using Eastep® qPCR Master Mix Kit (#LS2062, Promega, Madison, Wis, USA). Relative gene expression was calculated using the 2^{-ΔΔCt} method, with GAPDH as the reference gene. Standard techniques were used for protein quantification, separation, transfer, and blotting in ECC-1 and KLE cells. Primary antibodies against the following targets were used: TFEB (1:1000; #ab270604, Abcam, London, UK), ERRα (1:500; #ab137489, Abcam, London, UK), LPCAT1 (1:1000; #66044-1-Ig, Proteintech, Wuhan, China), LPCAT3 (1:1000; #67882-1-Ig, Proteintech, Wuhan, China), MMP2 (1:1000; #AF1420, Beyotime Biotechnology, Shanghai, China), Cortactin (1:1000; #AF2134, Beyotime Biotechnology, Shanghai, China), E-cadherin (1:1000; #3195, Cell Signaling Technology, Shanghai, China), vimentin (1:1000; #5741, Cell Signaling Technology, Shanghai, China), and GAPDH (1:2000; #60004-1-Ig, Proteintech, Wuhan, China).

Wound Healing

Cells were grown to confluence in 6-well plates, and a 200-μL tip was used to introduce a scratch in the monolayer. The scratch areas in the wells were washed with PBS and 1 mmol/L R-flurbiprofen until the cells in those areas were removed thoroughly and imaged at 0 and 24 h post-scratching. The horizontal migration rate was calculated using the following formula: (width 0 h – width 24 h)/width 0 h × 100%.

Chromatin-Immunoprecipitation (ChIP) assay

Cells were harvested followed by cross-linking for 10 min with 1% (v/v) formaldehyde. Afterward, cells were lysed by sonication. The cell lysates were immunoprecipitated with anti-TFEB (1:100; ab270604, Abcam, London, UK) overnight at 4 °C. After washing and elution, the crosslinks were reversed for 4 h at 65 °C. The eluted DNA was purified and analyzed by qPCR using a Bio-Rad SYBR Green intercalating fluorophore system with the following ERRα primers: 5'-AGT TGT GAG GAG CCT TTG GAC-3' (forward) and 5'-CGG TGG TAG CGA GCA GTT T-3' (reverse). The Ct value of each sample was normalized to the corresponding input value.

Luciferase reporter assays

Bioinformatics methods were used to analyze and predict the potential transcription factor binding sites in the ERRα promoter region. The ERRα promoter sequence (64,303,524 bp to 64,305,524 bp) relative to the transcription start site was amplified by PCR and inserted

into the pGL3-basic vector (#E1751, Promega, Madison, Wis, USA). KLE cells were cotransfected with empty pcDNA3.1 vector or TFEB-S211A pcDNA3.1 plasmid in 24-well plates with Lipofectamine 2000. After 48 h, the firefly and Renilla luciferase activities were measured using the Dual-Luciferase Reporter Assay Kit (#E1901, Promega, Madison, Wis, USA) and a microplate reader (Synergy H1, Bio-Tek, USA), and the ratio of firefly/Renilla luciferase activity was determined.

Lipid and metabolite profiling

Liquid chromatography mass spectrometry (LC/MS) analyses were performed using a high-performance liquid chromatography system (1260 series; Agilent Technologies, USA) and mass spectrometer (Agilent 6460; Agilent Technologies, USA). Briefly, 10⁷/ml EC cells or 20 mg EC tissue was homogenized in 1.5 mL of chloroform/methanol (2:1, v/v), vortexed for 1 min, centrifuged at 3,000 rpm for 10 min, added to 800 μ L organic phase in a clean tube, and dried with nitrogen. Sample preparation processes were performed in accordance with the above method of parallel preparation of quality control samples. Mass spectrometric analysis was conducted by adding 200 μ L isopropanol/methanol solution (1:1, v/v), and the supernatant was used for analysis. For targeted metabolomic analyses, multiple reaction monitoring transitions representing the metabolites were simultaneously monitored, and positive/negative polarity switching was used. Data analyses were performed according to the instructions of Shanghai Applied Protein Technology [20].

Tandem mass tag (TMT) labeling proteomics

The total protein in KLE cells and KLE^{XCT790} cells dealt with 10 μ M XCT790 were extracted and evaluated by SDS-PAGE and staining. The qualified protein samples were labeled with trypsin and TMT. The labeled polypeptides were mixed into one component in equal quantities. After desalination, high-pH HPLC was used for grading. Eight different polypeptide components were obtained, and each component was separated by nano-HPLC and detected by mass spectrometry. Then, maxQuant search software was used for protein identification and quantitative analysis. After the quantitative results were standardized, statistical analysis was conducted to screen out the differentially expressed proteins.

Mitochondrial stress detection

Mitochondrial stress detection was conducted by using the Seahorse XF Cell Mitochondrial Stress Test Kit (#103,015–100, Agilent, USA). In brief, the test solution based on DMEM medium (#103,575–100, Agilent, USA)

was heated in 37 °C and working solution was prepared for use. Oligomycin, 0.5 μ M FCCP, and rotenone/antimycin A were properly prepared into a working solution and added to the dole on the probe plate. Cell culture microplates were removed from a 37 °C CO₂ incubator, and the cells were examined under a microscope to confirm the 90% of confluence. Remove the test solution from the water bath. The cell growth medium in the cell culture microplates was replaced with preheated detection solution using a multichannel pipette, and the cell culture microplates were placed in a CO₂-free incubator at 37 °C for 1 h. Then, run the Seahorse XF 24 (Agilent, USA) on the computer and analyze the data.

Immunohistochemistry (IHC)

All tissues were assembled into a tissue microarray. Immunostaining for ERR α and TFEB was performed according to standard procedures. Rabbit polyclonal anti-ERR α (1:100; #ab137489, Abcam, London, UK) and rabbit polyclonal anti-TFEB (1:100; #ab270604, Abcam, London, UK) antibodies were used. The percentage of positive cells was scored as 0 (cells <5%), 1 (5% to 25%), 2 (26% to 50%), 3 (51% to 75%), and 4 (76% to 100%). The positive staining intensity was scored as 0 (no staining), 1 (weak staining), 2 (moderate staining), and 3 (strong staining). The expression levels of ERR α and TFEB were assessed to determine their immunoreactive scores (IRSs) using the algorithm IRS = Si \times Pi (where Si and Pi represent the intensity and percentage of positively stained cells, respectively). Samples were divided into four groups based on their IRS: 0, negative (-); 1–4, weakly positive (+); 5–8, positive (++) and 9–12, strongly positive (+++).

Scanning Electron Microscope (SEM)

Briefly, cells were cultured on petri dish and treated with electron microscopy fixative (#G1102, Servicebio, China). After post-fixing, dehydrate cells with 30%, 50%, 70%, 80%, 90%, 95% ethanol (#100,092,183, Sinaopharm Group Chemical Reagent Co. LTD, China) for 15 min, respectively. Dry samples with Critical Point Dryer. Specimens are attached to metallic stubs using carbon stickers and sputter-coated with gold for 30 s. Micrographs were revealed using HITACHI-SU8100 scanning electron microscope.

Participants and specimens

EC tissue and normal endometrial tissue samples and blood samples with relevant clinical data were obtained from surgical patients in Fujian Provincial Maternity and Child Health Hospital, Affiliated Hospital of Fujian Medical University from 2013 to 2018. None of the patients received any preoperative radiation, chemotherapy or

hormone therapy. Finally, we collected 111 tissue specimens, including 79 EC specimens and 32 normal endometrium specimens. The samples were embedded in paraffin, and all diagnoses of the pathological sections were made by experienced pathologists. In addition, according to ERR α immunoreactive scores, 35 cases with the highest score and 20 cases with the lowest score were selected for lipidomic analysis. Finally, because 1 EC tissue sample was missed (IRS = 7). A total of 51 patient tissues from 32 EC patients and 19 patients with normal endometrium were also collected for lipidomics analysis 3 samples were excluded because of metabolite degradation (Supplement Figure 1). All patients were informed of the experiments and signed informed consent forms. This research protocol was approved by the Ethics Committee of Fujian Provincial Maternity and Child Health Hospital, Affiliated Hospital of Fujian Medical University (No. FMCH-2018–14).

Statistical analysis

Statistical analysis was performed using GraphPad Prism 8.0 software and IBM SPSS (version 22). Statistical significance was determined by Student's *t* test or by ANOVA, and related parameters were analyzed using Pearson's correlation. Correlation coefficients for graded data were obtained using Pearson correlation analysis. Receiver operating characteristic (ROC) curves and the Youden Index were used to determine the cutoff point of continuous variables. Univariate binary logistic regression analyses were used to analyze indicators associated with EC. Differences with *p*-values less than 0.05 were considered significant.

Results

Bioinformatics analysis revealed that TFEB promotes ERR α transcription to participate in EC progression

To explore the role of TFEB and ERR α in EC, we first investigated the expression and clinicopathological data

of these two genes in 543 EC samples and 23 normal samples from TCGA RNA-seq database. High expression of TFEB was significantly associated with a more advanced stage ($p < 0.05$; Fig. 1A) but not with pathological grade in EC ($p > 0.05$; Fig. 1B). Moreover, EC patients with high expression of TFEB had worse overall survival (OS) than those with low expression ($p < 0.05$; Fig. 1C). Similarly, high ERR α expression was significantly associated not only with more advanced stages but also grades in EC (both $p < 0.05$; Fig. 1D-F). Consistent with our purpose, the expression of TFEB was significantly positively correlated with ERR α (Pearson coefficient = 0.168; $p < 0.001$; Fig. 1G).

ERR α is a direct transcriptional target of TFEB involved in lipid metabolism in EC

Previously, we demonstrated that the transcriptional activity of TFEB correlated with ERR α , but the exact mechanism remains unclear. Luciferase activity detection showed that the relative luciferase activity triggered by ERR α expression was significantly enhanced by the promotion of TFEB (Fig. 1H). To further study the crosstalk between TFEB and ERR α , ChIP-qPCR was performed, and the results confirmed that TFEB could directly bind to the promoter of ERR α DNA (Fig. 1I). Seven possible TFEB transcriptional binding sites (Fig. 1J); region P1-P7; all relative scores > 0.80) on the promoter region of the ERR α gene were predicted. Among them, the P5 site with the element sequence 3'-CGCACGTGGC-5' was the most likely combination with TFEB (Fig. 1J). These data strongly indicate that TFEB could directly bind to the ERR α promoter and positively regulate ERR α expression. ERR α is the key regulator involved in lipid catabolism. Gene set enrichment analysis (GSEA) of the high- and low-ERR α expression groups was conducted to explore and identify the potential function of ERR α in EC. The gene sets with nominal $p < 0.05$ and false discovery rate

(See figure on next page.)

Fig. 1 Bioinformatics analysis revealed that TFEB promotes ERR α transcription to participate in EC progression TCGA database (Sample size: Normal = 23; EC = 543) results are shown. **(A)** The expression of TFEB varies at different FIGO stages **(B)** and at different pathological grades. **(C)** The association of TFEB with OS in the patient/specimen quartiles is shown (Low: 1st quartile distribution; Median: 2nd-3rd quartile distribution; High: 4th quartile distribution). **(D)** The expression of ERR α varies at different FIGO stages **(E)** and at different pathological grades. **(F)** The association of ERR α with OS is shown. **(G)** The correlation between the expression levels of TFEB and ERR α in EC tissue. **(H)** ChIP analysis of the ERR α promoter occupancy in KLE cells is performed as described in the Materials and Methods section. TFEB is immunoprecipitated using an anti-Flag antibody, and DNA enrichment is performed using qPCR. The ATP6V1H promoter is used as a positive control and the GLA promoter is used as a negative control. **(I)** KLE cells are co-transfected with Flag-TFEB, ERR α promoter labeled with Luciferase reporter, and Renilla luciferase control. 48 h after transfection, the cells are analyzed and the relative luciferase activity is measured and normalized to the Renilla luciferase control. **(J)** The putative ERR α -binding sites (ERR α s), as predicted by the online program JASPAR (<https://jaspar.genereg.net/analysis>), are located in the TFEB (P1-P7) gene promoter regulatory regions. **(K)** KEGG pathway analysis (Ordinate: the KEGG signal path; abscissa: enrichment score). Results of GSEA in fatty acid metabolism and adipogenesis pathways. **(L)** The association of fatty acid metabolism and adipogenesis with tumor invasion is shown (Low: 1st-2nd quartile distribution; High: 3rd-4th quartile distribution). Statistical tests: ANOVA (A-B, D-E), Kaplan–Meier estimator (C, F), Pearson correlation analysis (G), and Student's *t*-test (L). $p < 0.05$ suggests significantly different. TCGA: The Cancer Genome Atlas; FIGO: Federation International of Gynecology and Obstetrics; OS: Overall Survival; ChIP: Chromatin Immunoprecipitation; KEGG: Kyoto Encyclopaedia of Genes and Genomes; GSEA: Gene Set Enrichment Analysis.

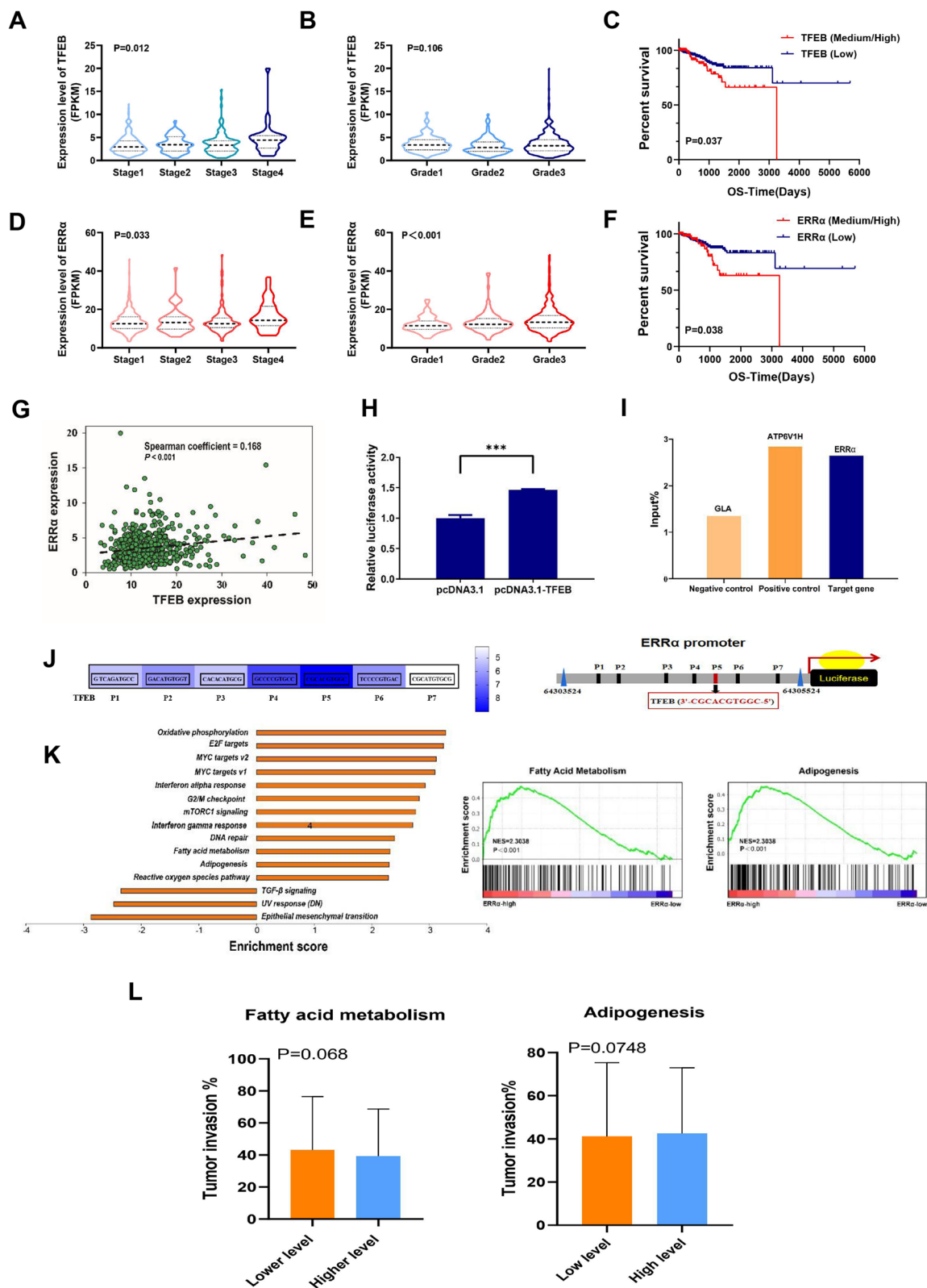


Fig. 1 (See legend on previous page.)

(FDR) < 0.25 were considered significantly enriched in fatty acid (FA) metabolism and adipogenesis (Fig. 1K). Then, we found FA metabolism and adipogenesis pathway both were nearly significantly associated with tumor invasion ($p=0.068$ and $p=0.075$, respectively, Fig. 1L), which suggested that lipid metabolism might play an important role in the invasion of EC.

ERR α elevated unsaturated fatty acid (UFA)-containing GPs in EC

Subsequently, lipidomics was performed and analyzed in KLE^{TFEB-OV} cells and KLE^{ERR α -OV} cells. In general, 7 categories of lipids, which were composed of 1120 glycerophospholipids (GPs), 345 sphingolipids (SPs), 285 glycerolipids (GLs) and other lipid categories, were screened and identified based on a LC-MS/MS system (Fig. 2A). Finally, 36 classes of lipids were tested, which included 395 phosphatidylcholines (PCs), 252 triacylglycerols (TAGs), 236 phosphatidylethanolamines (PEs) and other lipid species (Fig. 2B). Systematic lipidomic changes occurring between KLE^{TFEB-OV} and KLE^{ERR α -OV} were then assessed by orthogonal partial least squares-discriminant analysis (OPLS-DA). There was obvious heterogeneity both in KLE^{TFEB-OV} and KLE^{ERR α -OV} with $R^2Y=0.994$, $Q^2=0.910$ and $R^2Y=0.989$, $Q^2=0.838$, respectively (Fig. 2C-D). Lysophosphatidylethanolamine (LPE), diglyceride (DG), coenzyme (Co) and wax esters (WE) was observed to decrease remarkably in KLE^{TFEB-OV}. And digalactosyldiacylglycerol (DGDG) was observed to increase statistically, while gangliosides2 (GM2) was reduced significantly in KLE^{ERR α -OV}. Although PC and sphingomyelin (SM) changed with TFEB or ERR α elevation indistinctly, the ratio of PC/SM was distinctly increased both in KLE^{TFEB-OV} and KLE^{ERR α -OV}, which was used to evaluate cell membrane fluidity ($p<0.05$, Fig. 2E-F).

As the direct target of TFEB, ERR α obviously elevates 7 species of lipids, including PCs, phosphatidylglycerols (PGs), cardiolipins (CLs), PE (18:1/20:5), phosphatidylserines (PSs) and ceramides (Cers). Increased UFA-containing PCs, PGs, PSs, SMs, CLs and PE (18:1/20:5) and a decrease in saturated fatty acid (SFA)-containing PCs, PGs and SM (40:0) were also detected in KLE^{ERR α -OV} (Fig. 2G). Moreover, the overlapping lipids of KLE^{TFEB-OV} and KLE^{ERR α -OV} were PC (35:1)+H, PC (36:3)+H and PG (18:1/22:6)+H, respectively (Supplement Table 1). In brief, the common event is that UFA-containing GPs

are increased in ERR α -overexpressing EC cells. The data showed that the membrane fluidity of KLE was increased with ERR α . Hence, TFEB drives ERR α to elevate the unsaturation of fatty acyl moieties in GPs, which enhances membrane fluidity for invasion and metastasis.

Proteins/lipids related to ERR α were enriched in mitochondrial function in EC

Compared to control KLE cells, 173 proteins related to ERR α with unique peptides ≥ 2.0 , FC > 1.3 and $p < 1.0$ were gained in KLE cells treated with XCT790. The biological process of these proteins was mainly enriched in mitochondrial function, and the cell component was enriched in cone filopodium growth (Fig. 3A). Since an identified potential biological process was found to be affected by ERR α , the concentrations of these proteins/lipids were next evaluated in EC invasion and metastasis. Thirty-two proteins were significantly different between UFA-containing PCs, PGs, SMs and SFA-containing PCs, PGs, and SMs by combining proteomics and lipidomics (Fig. 3B-C, Supplement Table 2). The mitochondrial function was mainly enriched by STRING analysis (Fig. 3D). Then, we routinely detected genes associated with FA metabolism, including *acc*, *fasn* and *acadm*, which showed that FA metabolism was dynamic. Generally, all the genes were upregulated as TFEB-ERR α increased and downregulated as TFEB-ERR α decreased in KLE and ECC-1 cells (Fig. 4A). Subsequently, mitochondrial stress was evaluated by an energy analyzer. Compared to that of their controls, the maximum oxygen consumption rate (OCR) of cells treated with 0.5 μ M FCCP was increased in KLE^{TFEB-OV} and KLE^{ERR α -OV}, which was decreased in KLE^{TFEB-KD} and KLE^{ERR α -KD} cells ($p < 0.05$). The OCR related indicators, including basal, maximal respiration, and spare respiratory capacity were significantly higher in KLE^{TFEB-OV} and KLE^{ERR α -OV} cells ($p < 0.05$). Meanwhile, in KLE^{TFEB-KD} and KLE^{ERR α -KD} cells, the decreasing level of basal, maximal respiration, and spare respiratory capacity was also showed ($p < 0.05$). Moreover, the level of ATP also showed a positive correlation of TFEB and ERR α ($p < 0.05$). A similar trend was observed in ECC-1 cells. To further confirm the effects of TFEB on ERR α -mediated mitochondrial stress, ERR α levels were inhibited in KLE^{TFEB-OV} cells and ECC-1^{TFEB-OV} after XCT790 treatment. The OCR was no significant increase in KLE^{TFEB-OV+XCT790} cells and ECC-1^{TFEB-OV+XCT790} cells ($p > 0.05$; Fig. 4B).

(See figure on next page.)

Fig. 2 ERR α elevated unsaturated fatty acid (UFA)-containing GPs in EC (A) Seven subgroups of lipids in KLE cells are detected using lipidomics. (B) 36 classes of lipids were tested in KLE cells. (C) Systematic lipidomic changes between KLE and KLE^{TFEB-OV} assessed by orthogonal partial least squares-discriminant analysis (OPLS-DA). (D) Systematic lipidomic changes between KLE and KLE^{ERR α -OV} assessed by OPLS-DA. (E) Significant lipid species associated with TFEB and its PC/SM evaluation. (F-G) Significant lipid species associated with ERR α and its PC/SM evaluation. ($p < 0.05$ and VIP > 1 indicate significant). *, $p < 0.05$. Statistical tests: Student's t-test. TFEB-OV: TFEB Over-Expressed; ERR α -OV: ERR α Over-Expressed.

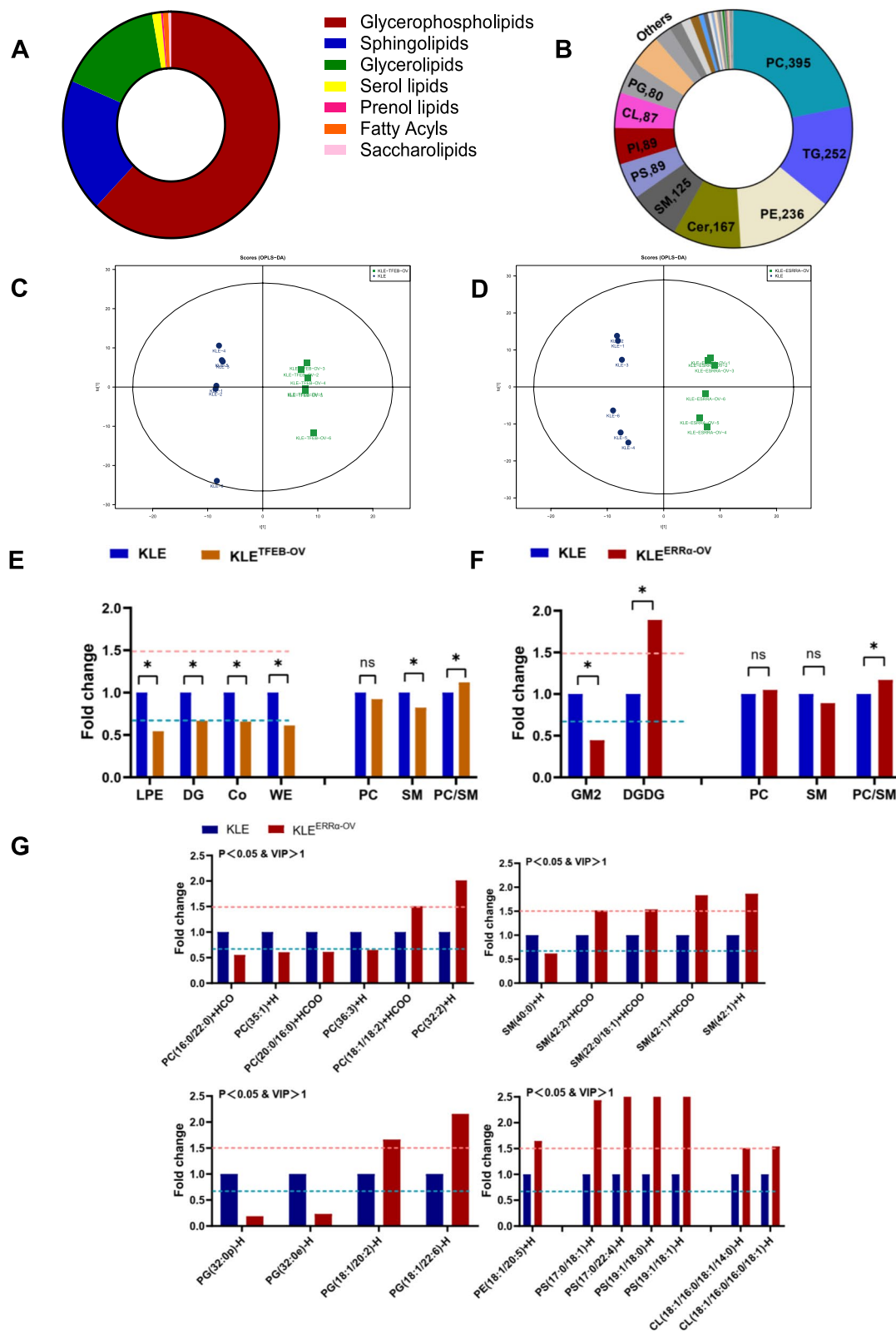


Fig. 2 (See legend on previous page.)

The degree of saturation of fatty acyl moieties of membrane phospholipids determines the biophysical properties of cell membranes, such as their fluidity. LPCAT1 and LPCAT3 are the key phospholipid remodeling enzymes that regulate the degree of saturation of fatty acyl moieties in the membrane [16]. Thus, we tested the FA desaturase proteins LPCAT1 and LPCAT3. LPCAT1/3 were increased in KLE^{ERR α -OV} compared with the controls. In contrast, both LPCAT1 and LPCAT3 decreased in KLE^{ERR α -KD} compared with the controls ($p < 0.05$). Similarly, MMP2 and Cortactin were altered with ERR α which detected to evaluate membrane fluidity ($p < 0.05$; Fig. 4C). A similarly trend of LPCAT1/3, MMP2 and Cortactin was observed in ECC-1 cells. Furthermore, LPCAT1/3, MMP2 and Cortactin were inhibited apparently when we treated KLE and ECC-1 with XCT790. However, these proteins could not be reversed by XCT790 when TFEB was over-expressed ($p < 0.05$; Fig. 4D). To observe the generation of pseudopod, we found there were more filopodia in KLE^{TFEB-OV} and KLE^{ERR α -OV} than KLE cells, while fewer thin filopodia were scanned in KLE^{ERR α -KD} and KLE with XCT790 treatment by SCE. Moreover, TFEB over-expressed annulled the inhibitory effect of XCT790 to keep the filopodia and pseudopod. Consistent with KLE cell pseudopodia, TFEB-ERR α promote the filopodia and the outcome of XCT790 treatment could be withdrew as TFEB was up-regulated. (Fig. 4E) These data suggested that TFEB could induce mitochondrial stress and phospholipid remodeling to elevate the fluidity of the cell membrane by upregulating ERR α in KLE and ECC-1 cells.

TFEB promotes EC migration depending on ERR α via EMT signaling

Although the role of ERR α in promoting EC invasion and metastasis has been established [9], its underlying mechanisms are far from elucidated. The migration ability of KLE and ECC-1 cells was remarkably changed after regulation of the expression of TFEB or ERR α through a lentivirus-mediated strategy. Compared to the controls, the scratched spaces were up to 47.2% in KLE^{TFEB-OV}, 21.9% in KLE^{ERR α -OV} at 24 h and up to 126.4% in ECC-1^{TFEB-OV}, respectively (both $p < 0.05$; Fig. 5A-B). The scratched spaces of ECC-1^{ERR α -OV} at 24 h also increased slightly, but there was no significant difference from their controls ($p > 0.05$). The wounded spaces were nearly two-fold decreased at 24 h in both KLE^{TFEB-KD} and KLE^{ERR α -KD} cells compared with their

controls ($p < 0.001$). A similar trend was observed in ECC-1^{TFEB-KD} and ECC-1^{ERR α -KD}. To further confirm the effects of TFEB on ERR α -mediated cell migration, ERR α levels were inhibited in KLE^{TFEB-OV} cells and ECC-1^{TFEB-OV} cells after XCT790 treatment. The scratched space was not significantly increased from 0 to 24 h in KLE^{TFEB-OV+XCT790} cells or ECC-1^{TFEB-OV+XCT790} cells. Meanwhile, the enhanced migration abilities of KLE^{TFEB-OV} and ECC-1^{TFEB-OV} cells were partially compromised after XCT790 treatment ($p < 0.05$; Fig. 5A-B). Moreover, the RT-qPCR results showed that downregulation of TFEB reduced the expression of ERR α and vimentin and increased the expression of E-cadherin in ECC-1 and KLE cells. In contrast, TFEB overexpression enhanced the expression of ERR α and vimentin and decreased the expression of E-cadherin ($p < 0.05$, Fig. 5C-D). These data are similar to the findings observed in Western blot experiments ($p < 0.05$, Fig. 5E). Importantly, there was no significant change in ERR α , vimentin or E-cadherin expression when KLE^{TFEB-OV} and ECC-1^{TFEB-OV} cells were treated with 10 μ M XCT790 ($p > 0.05$, Fig. 5F). This demonstrated that TFEB could regulate cell migration in an ERR α -dependent manner via the EMT signaling pathway.

High expression of TFEB-ERR α is associated with dyslipidemia and metastasis in EC patients

To verify the results obtained above, IHC was performed on an EC tissue microarray (TMA), which included 79 EC specimens and 32 normal endometrium specimens. Positive immunoreactivity for TFEB was detected in the nuclei of both carcinoma cells and normal endometrial gland cells. Significantly higher immunoreactivity was observed in EC tissue than in normal endometrial tissue ($p < 0.001$; Fig. 6A & Table 1). Similarly, ERR α could also be detected in 79 EC tissue samples with a higher immunoreactivity than it detected in 32 normal endometrial tissues ($p < 0.001$; Fig. 6A & Table 1). There was no significant difference in TFEB or ERR α expression among EC patients with different International Federation International of Gynecology and Obstetrics (FIGO) stages, histologic tumor grades, pathological types or lymph node metastasis (LNM) conditions ($p > 0.05$; Fig. 6C). However, significant differences were detected between the $\leq 1/2$ and $> 1/2$ myometrial invasion (MI) groups for both TFEB and ERR α expression in EC patients ($p < 0.05$; Fig. 6C). Moreover, a positive correlation between TFEB and ERR α immunoreactivity

(See figure on next page.)

Fig. 3 Proteins/lipids related to ERR α were enriched mitochondrial function of EC (A) Enrichment analysis for canonical pathways (CP) and biofunctions (BF) was performed on proteins related to ERR α . (B) 173 proteins related to ERR α were gained in KLE cells treatment with 10 μ M XCT790 for 24 h using proteomics. (Blue, down-regulated; Red, up-regulated) (C) The significant protein related to the degree of unsaturated lipids were analyzed by STRING. (D) Mitochondrial function and glucolipid metabolism were enriched by GO and KEGG.

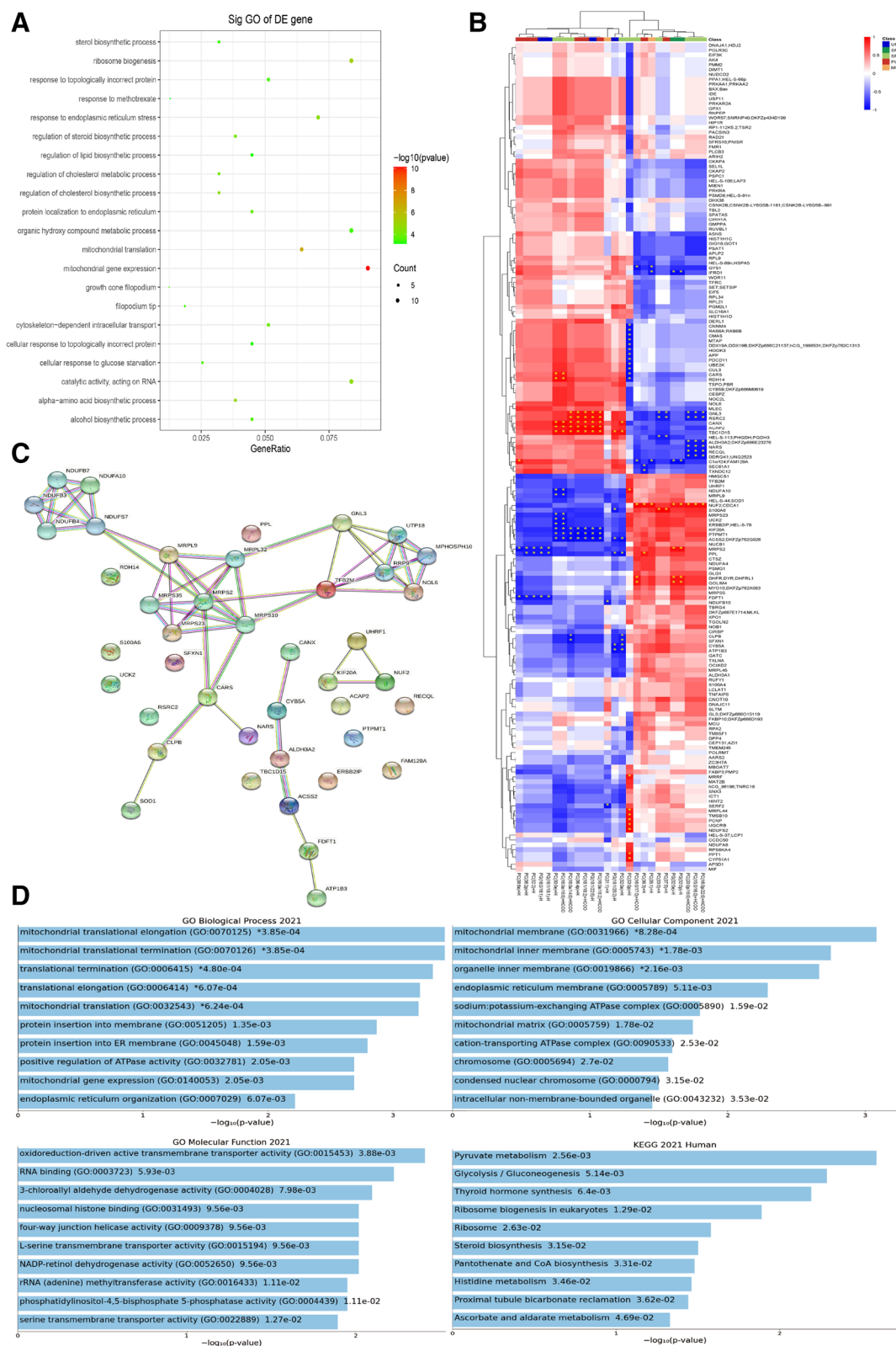


Fig. 3 (See legend on previous page.)

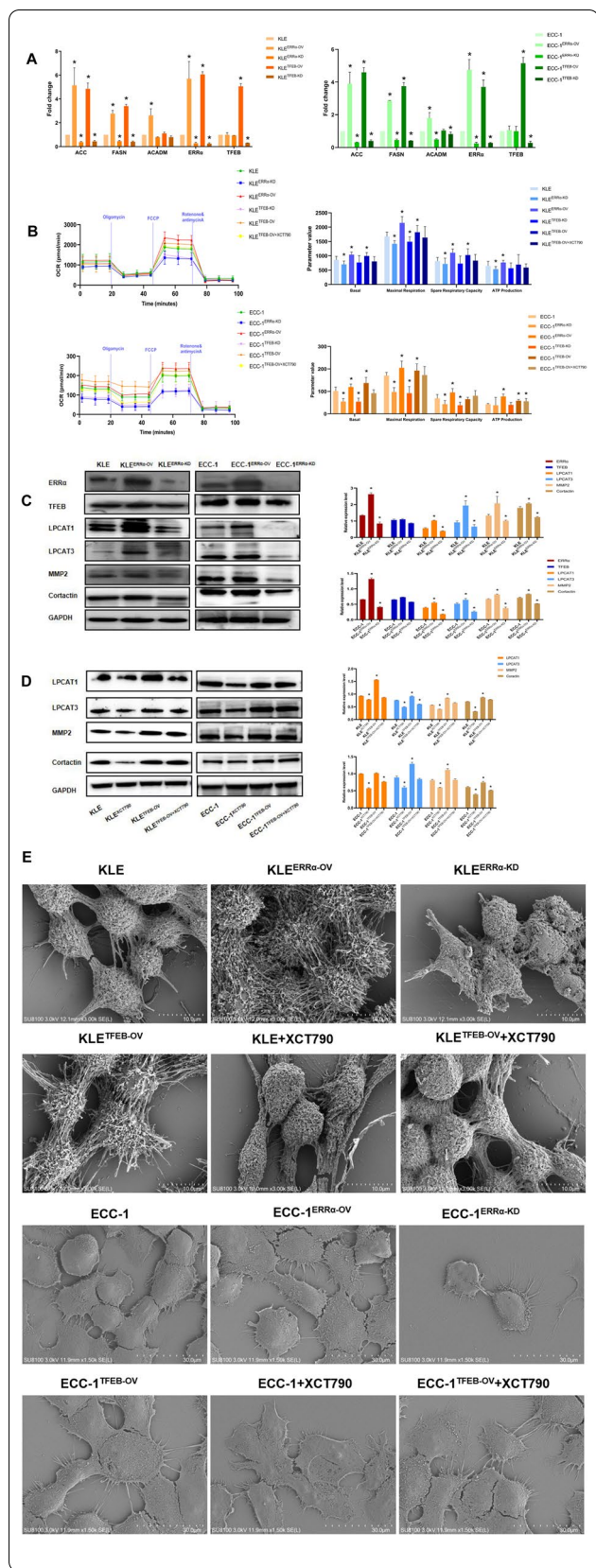


Fig. 4 Proteins/lipids related to ERRα were enriched in mitochondrial function in EC (A) The relationship between TFEB-ERRα and *acc*, *fasn*, *acadm* are determined by RT-qPCR in KLE and ECC-1 cells. (B) The association of oxygen consumption rates (OCR), basal, maximal respiration, spare respiratory capacity, and ATP production regulated by TFEB-ERRα are shown. (C) The effect of ERRα regulation on TFEB, LPCAT1, LPCAT3, MMP2, and Cortactin expression in EC cells is analyzed using western blot (WB). (D) The effect of XCT790 treatment on LPCAT1, LPCAT3, MMP2, and Cortactin proteins for 24 h were evaluated between control and TFEB-overexpressing by WB. (E) Representative Scanning electron microscope (SEM) micrographs of KLE and ECC-1: TFEB-ERRα axis and XCT790 treatment for 24 h regulated pseudopod, in comparison to the controlled group. Micrographs are screened at scale of 10–30 μM. *, p < 0.05. Statistical tests: Student’s t-test or ANOVA.

was found based on Pearson’s rank correlation analysis ($r = 0.642$, $p < 0.001$, Fig. 6B).

Interestingly, in a study on the same population for serum lipids, the serum total triglyceride (TG) level was significantly higher, while the high-density lipoprotein (HDL) and apolipoprotein A (APO-A) levels were significantly lower in EC patients than in health people ($P < 0.05$, Table 1). In addition, the low-density lipoprotein (LDL) level was obviously higher in patients with endometrioid endometrial cancer (EEC) than in patients with non-endometrioid endometrial cancer (NEEC). Importantly, both HDL and APO-A levels were decreased significantly in patients with LNM ($p < 0.05$, Table 1). Next, we compared the differences in serum lipids in populations with different TFEB/ERRα expression levels. Not unexpectedly, serum HDL and APO-A levels were much lower in the patients with high expression of TFEB and ERRα (+ + / + +) than in those with low TFEB and ERRα expression (- / +) ($p < 0.05$; Fig. 6D). Given from the evidence above, elevated TFEB-ERRα is involved in EC invasion and metastasis and is related to decreases in serum HDL and APO-A levels.

Accumulation of UFA-containing GPs induced by ERRα is required for EC progression

The species of lipids obtained from 32 cases of EC tissues and 19 cases normal endometrial tissues (3 cases were disqualified) were similar to the cells, which included 359 PCs, 324 TAGs, 269 PEs and other lipid species (Fig. 7A-B). Venn showed that 2 lipids were found in three groups, including PG (18:1/22:6)+H, PC (36:3)+H and 19 lipids were detected both in KLE^{ERRα-OV} and clinical tissues (Fig. 7C). Systematic lipidomic changes occurring between EC patients and normal controls were assessed by OPLS-DA. There was obvious heterogeneity between the populations, with $R^2Y = 0.963$ and $Q^2 = 0.510$ (Fig. 7D). Fair discrimination was also found between patients with LNM

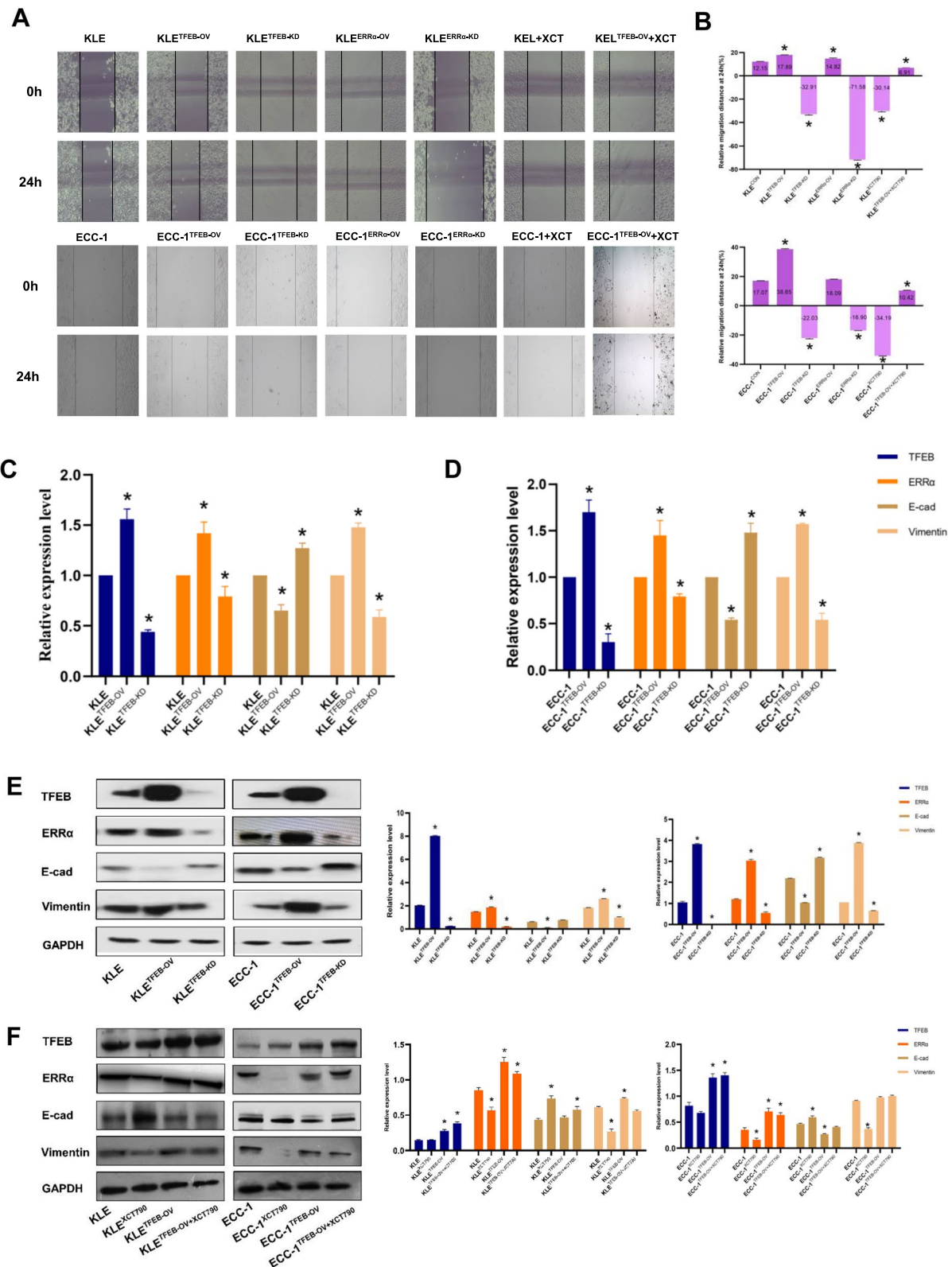


Fig. 5 TFEB promotes EC migration depending on ERRα via EMT signaling (A-B) Wound healing of TFEB-ERRα regulation in KLE and ECC-1 cells. (C-D) TFEB regulates ERRα, E-cadherin, and vimentin expression in EC cells is analyzed using RT-qPCR. (E-F) The effect of XCT790 treatment for 24 h on TFEB over-expressing in EC cells. *, p < 0.05. Statistical tests: Student's t-test.

($n=8$) and those without LNM ($n=24$). ($R^2Y=0.789$ and $Q^2=0.574$, Fig. 7E). Consistent with the results from in vitro research in cells, DGDG was observed to increase with a fold change (FC) >1.5 . In addition, PGs, including phosphatidylinositol (PI), lysophosphatidylserine (LPS), lysophosphatidylethanolamine (LPE) and PG, sphingolipids (SLs), including Hex2Cer, Hex1Cer, Cer and ceramide phosphate (CerP), and GLs, including monoglyceride (MG) and TG, were also increased in EC tissue. Although SM was elevated indistinctively, PC/SM was significantly increased in EC tissue, which was used to evaluate cell membrane fluidity ($p<0.05$, Fig. 7F). Moreover, UFA-containing GPs, such as PC (18:1/18:2)+HCOO, PC (32:2)+H, PG (18:1/22:6)+H and SM (42:1)+HCOO, were obviously increased in EC tissue compared to normal endometrium (FC >1.5 , VIP >1 and $p<0.05$; Fig. 6F). However, compared to patients without LNM, PC (18:1/18:2)+HCOO was much higher in the patients with LNM ($p<0.05$; Fig. 7G). We performed ROC curve analysis and obtained the cut-off values. The results showed that PC (18:1/18:2)+HCOO and CA125 have good diagnostic value in patients with advanced-stage EC ($p<0.05$; Supplement Figure 2). Moreover, PC (18:1/18:2)+HCOO was found to be an independent risk factor for EC patients in advanced stage by univariate binary logistic regression analyses ($p<0.05$, Fig. 7H).

Furthermore, we compared the differences in serum lipids in populations with different PC (18:1/18:2)+HCOO expression levels. The results showed that the serum HDL level was much lower in the patients with higher expression of PC (18:1/18:2)+HCOO than in those with lower PC (18:1/18:2)+HCOO ($p<0.05$, Table 2). Moreover, a positive correlation between PC (18:1/18:2)+HCOO and ERR α immunoreactivity was found based on Pearson's rank correlation analysis ($r=0.805$, $p<0.001$, Fig. 7I). These results suggested that increased PC (18:1/18:2)+HCOO induced by ERR α was a novel biomarker of EC progression, which was probably related to the decrease in serum HDL.

In conclusion, the TFEB-ERR α axis promotes UFA-containing GP accumulation to induce lipid reprogramming hallmarked by mitochondrial stress, which contributes to the invasion and metastasis of EC (Supplement Figure 3). Importantly, UFA-containing PC, SM and PG were the significantly altered lipids found in EC cells and tissues, among which, PG (18:1/22:6)+H induced by

TFEB-ERR α axis was involved in tumorigenesis and PC (18:1/18:2)+HCOO was the ERR α -dependent lipid to mediate EC metastasis.

Discussion

EC is one of the cancers most related to metabolic disorders, and patients present with hyperlipidemia, hyperglycemia, hypertension and other clinical symptoms [21]. Guo et al. suggested that metformin significantly reversed obesity-driven lipid and protein biosynthesis upregulation in an obese LKB1^{fl/fl} p53^{fl/fl} mouse model of EC [22]. Recently, an increasing number of studies have confirmed that ERR α is a key regulator of metabolism in obesity-related tumors, such as breast cancer [23], prostate cancer [24], and EC [25]. Moreover, ERR α -mediated signaling pathways have recently emerged as key factors in the regulation of cancer lipid metabolism. In our previous work, the translational factor activity of TFEB was affected by the downregulation of ERR α expression in EC according to a high-throughput DNA/protein assay [25], which suggested that TFEB should interact with ERR α and be involved in EC lipid reprogramming and progression, which triggered our interest. TFEB downregulation or deficiency can obviously affect the cellular phenotype in a physiologically relevant manner in settings including atherosclerosis [26], nonalcoholic fatty liver disease [27], cancer [28] and neurodegeneration [29]. Furthermore, TFEB is activated by starvation or caloric restriction and plays roles in lipid catabolism and lysosomal biogenesis [14]. Therefore, we started with bioinformatics analysis of the TCGA data. In agreement with our hypothesis, the results confirmed that both TFEB and ERR α are strongly associated with a poor prognosis in EC, as reflected by their associations with a high FIGO stage and a shortened survival time. Moreover, the expression of TFEB was first found to be positively correlated with the expression of ERR α in the TCGA data of 543 EC cases. The bioinformatics analysis result was further verified by our clinical data from our TMA, in which TFEB and ERR α showed a strong correlation and both were related to the MI of EC. However, the exact interaction mechanism between TFEB and ERR α has not yet been described clearly. In 2019, TFEB was reported to drive PGC-1 α expression in adipocytes to protect against diet-induced metabolic dysfunction, while PGC-1 α is one of the most important coactivators of ERR α [30]. We further confirmed that

(See figure on next page.)

Fig. 6 High expression of TFEB-ERR α is associated with dyslipidemia and metastasis in EC patients The immunohistochemical expression of several proteins and their correlations are shown. **(A)** The immunohistochemical expression of TFEB and ERR α in the normal endometrium ($n=32$) and EC at different FIGO stages ($n=79$) (magnification: $\times 400$). **(B)** The correlation between TFEB and ERR α expression is shown in tissues. **(C)** Analysis of TFEB-ERR α and clinicopathological features. **(D)** The differences level of serum TG, HDL, APOA and LDL in groups with different expression levels of TFEB. *, $p<0.05$. Statistical tests: Student's t-test (D), Pearson's rank correlation analysis (C). MI: Myometrial Invasion; LNM: Lymph Node Metastases; TG: Triglyceride; HDL: High-Density Lipoprotein; APOA: Apolipoprotein A; LDL: Low-Density Lipoprotein.

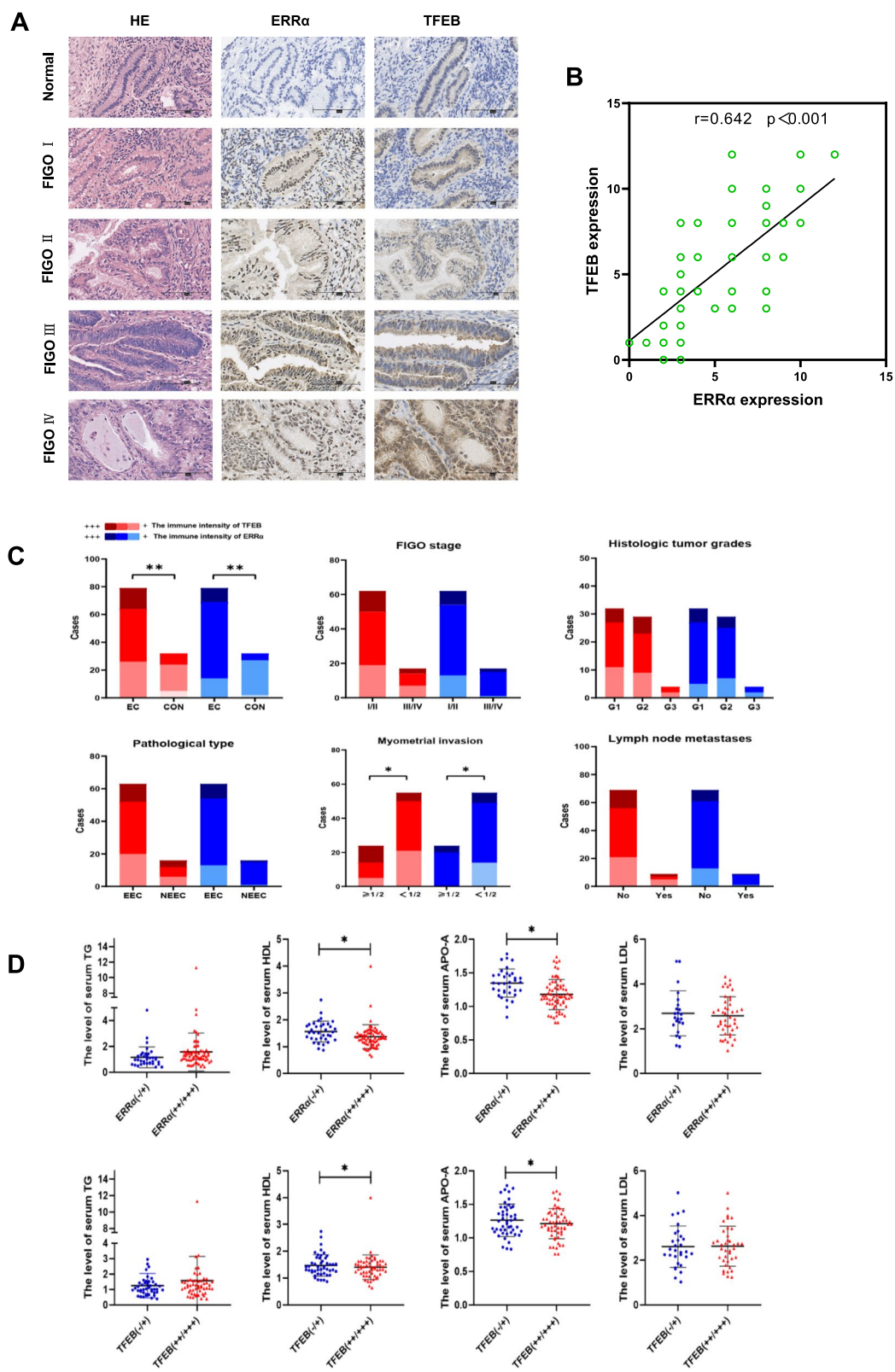


Fig. 6 (See legend on previous page.)

Table 1 The level of serum lipid, ERRα and TFEB in tissue microarray of EC patients and controls

| Parameter (N=111) | TG | P | CHOL | P | HDL | P | APO-A | P | LDL | P | APO-B | P | TFEB | | | | ERRα | | | |
|------------------------|-------------|--------------|-------------|-------|-------------|--------------|-------------|--------------|-------------|--------------|-------------|-------|------|----|-----|------------------|------|----|-----|------------------|
| | | | | | | | | | | | | | -/+ | ++ | +++ | P | -/+ | ++ | +++ | P |
| Normal (n=32) | 1.027±0.882 | 0.032 | 4.623±0.853 | 0.649 | 1.599±0.412 | 0.041 | 1.331±0.229 | 0.026 | 2.709±0.830 | 0.568 | 0.834±0.229 | 0.157 | 24 | 8 | 0 | <0.001 | 27 | 5 | 0 | <0.001 |
| EC (n=79) | 1.549±1.369 | | 4.723±1.032 | | 1.394±0.428 | | 1.207±0.226 | | 2.578±0.929 | | 0.924±0.338 | | 26 | 38 | 15 | | 14 | 55 | 10 | |
| Stage I-II (n=62) | 1.556±1.538 | 0.859 | 4.703±1.133 | 0.192 | 1.388±0.470 | 0.980 | 1.191±0.224 | 0.691 | 2.693±0.985 | 0.178 | 0.935±0.381 | 0.785 | 19 | 31 | 12 | 0.710 | 13 | 41 | 8 | 0.328 |
| Stage III-IV (n=17) | 1.622±1.019 | | 5.055±0.719 | | 1.386±0.234 | | 1.218±0.210 | | 3.148±0.636 | | 0.958±0.236 | | 7 | 7 | 3 | | 1 | 14 | 2 | |
| MI <50% (n=55) | 1.597±1.531 | 0.589 | 4.742±1.064 | 0.806 | 1.388±0.463 | 0.827 | 1.196±0.219 | 0.550 | 2.593±0.979 | 0.880 | 0.936±0.362 | 0.618 | 21 | 29 | 5 | 0.003 | 14 | 35 | 6 | 0.024 |
| MI ≥ 50% (n=24) | 1.445±0.933 | | 4.680±0.979 | | 1.408±0.350 | | 1.231±0.244 | | 2.553±0.869 | | 0.898±0.282 | | 5 | 9 | 10 | | 0 | 20 | 4 | |
| EEC (n=63) | 1.515±1.397 | 0.592 | 4.790±1.056 | 0.184 | 1.424±0.452 | 0.120 | 1.218±0.225 | 0.390 | 2.706±0.976 | 0.021 | 0.950±0.353 | 0.100 | 20 | 32 | 11 | 0.613 | 13 | 41 | 9 | 0.216 |
| NEEC (n=16) | 1.711±1.256 | | 4.412±0.887 | | 1.274±0.301 | | 1.162±0.232 | | 2.133±0.578 | | 0.819±0.254 | | 6 | 6 | 4 | | 1 | 14 | 1 | |
| LNM (n=9) | 1.605±1.447 | 0.316 | 4.724±1.059 | 0.729 | 1.367±0.421 | 0.046 | 1.193±0.223 | 0.151 | 2.640±0.946 | 0.092 | 0.925±0.351 | 0.984 | 5 | 2 | 2 | 0.232 | 1 | 7 | 1 | 0.842 |
| No-LNM (n=70) | 1.413±0.380 | | 4.836±0.812 | | 1.637±0.439 | | 1.326±0.242 | | 1.980±0.666 | | 0.923±0.253 | | 21 | 36 | 13 | | 13 | 48 | 9 | |

Abbreviations: APO-A Apolipoprotein A, APO-B Apolipoprotein B, CHOL Cholesterol, ERRα Estrogen-Related Receptor α, EC Endometrial Cancer, EEC Endometrioid Endometrial Cancer, HDL High-Density Lipoprotein, LDL Low-Density Lipoprotein, LNM Lymph Node Metastasis, MI Myometrial Invasion, NEEC Non-Endometrioid Endometrial Cancer, TG total Triglyceride, TFEB Transcription Factor EB. p < 0.05 suggests significantly different

TFEB can bind to the promoter region of $ERR\alpha$ and regulate the expression and function of $ERR\alpha$ in vitro by ChIP assay and luciferase assay.

Previously, we reported that high expression of $ERR\alpha$ is associated with cancer cell metastasis and invasion [11]. To our knowledge, this is the first report indicating that TFEB participates in the invasion of EC cells by EMT signaling. Interestingly, the patient's clinical lipid profile indicated that serum HDL and APO-A were negatively correlated with TFEB and $ERR\alpha$. Lower serum HDL and APO-A levels were associated with LNM in EC patients. As we know, PC was the major phospholipids of HDL [31]. Importantly, we found a significant decrease in HDL in the patients with higher PC (18:1/18:2)+HCOO, which indicated that PC remodeling probably influenced the serum HDL level of EC patients. Together, TFEB/ $ERR\alpha$ was an early predictor of MI, while lower HDL/APO-A and higher PC (18:1/18:2)+HCOO were risk factors for LNM in advanced EC. In brief, TFEB/ $ERR\alpha$ regulates EC patients' lipid metabolism and is involved in EC invasion and metastasis.

Moreover, our in vitro and in vivo lipidomics experiments first investigated $ERR\alpha$ as a downstream signal by which TFEB promotes UFA-GP accumulation during EC progression. Guo found dramatic increases in lipid biosynthesis and lipid peroxidation in a genetically engineered mouse model of endometrioid adenocarcinoma [22], suggesting that lipidomic changes or reprogramming are significant in EC. Previous studies have confirmed that downregulation of $ERR\alpha$ provides a potential therapeutic strategy and inhibits cellular metastasis and invasion in EC [11, 25]. However, the mechanism by which TFEB- $ERR\alpha$ regulates FA and GP synthesis was unexplored prior to our study. After overexpressing TFEB and $ERR\alpha$, the top three categories of lipids obtained were GPs, SPs and GLs. Among them, PC (36:3)+H, PC (35:1)+H and PG (18:1/22:6)+H were found to be the significantly lipids and PG (18:1/22:6)+H was the lipid positively related to TFEB- $ERR\alpha$ overexpression, which was also elevated in cancerous tissues. This evidence indicated an unexpected role of TFEB- $ERR\alpha$ in FA unsaturated and phospholipid remodeling pathways that are controlled by

rate-limiting metabolic enzymes, including LPCAT1 and LPCAT3 [32, 33]. The impacts of UFA-containing GP accumulation on membrane fluidity have been proposed as secondary effects linked to desaturation induced by LPCAT1 and LPCAT3. The sensitivity of lipids to oxidative stress depends on their fatty acid moiety. Double bonds in MUFAs and PUFAs show a prevalent *cis* conformation, which produces bends and limits their rigid packing [34]. Since double bonds make fatty acyl chains more susceptible to oxidative stress, increased UFA-GPs promote membrane fluidity when ATP is elevated in this study. Commonly cancer cells possess different and complementary metabolic profiles, microenvironments and adopting behaviors to generate more ATPs to fulfill the requirement of high energy, which is further utilized in the production of proteins and other essential processes required for cell survival, growth, and proliferation. Mitochondria are partially autonomous organelles that depend on the import of certain proteins and lipids to maintain cell survival and membrane formation [35]. CL and/or PG are considered mitochondria-specific phospholipids [36]. PG (18:1/22:6) was found to be increased in MYC-induced T cell acute lymphoblastic leukemia, renal cell carcinoma, hepatocellular carcinoma, and lung carcinoma [37]. Our results showed that PG (18:1/22:6)+H was much higher in EC patients, which demonstrated the important role of mitochondria in maintaining membrane homeostasis. The synthesis of mitochondrial ATP plays a key role in inducing membrane curvature to establish cristae in eukaryotes [38]. The effect of mitochondrial stress was considered as the hallmark of membrane remodeling, which demonstrated herein that TFEB- $ERR\alpha$ enhanced membrane fluidity by stimulating mitochondria to prepare for invasion and metastasis. However, mitochondria lacks PC synthesizing enzymes, and this lipid has to be imported from other organelles, such as the endoplasmic reticulum (ER). The prevailing view is that a significant pool of cellular PC can also be made de novo from PS in a pathway that originates in the ER and passes into and out of the mitochondrion [39]. The genes related to FA metabolism, such as *acc*, *fasn* and *acadm*, increased with $ERR\alpha$, which suggested that $ERR\alpha$ mobilized β -oxidation and de novo lipogenesis to facilitate lipid reprogramming.

(See figure on next page.)

Fig. 7 Accumulation of UFA-containing GPs induced by $ERR\alpha$ is required for EC progression **(A)** The baseline characteristic including BMI, menopause, FIGO stage, histologic type, MI, LNM and $ERR\alpha$ expression of patients (EC = 35 vs controls = 19) tissues for lipidomic. **(B)** Different classes of lipids were tested in 35 EC tissues and 19 control tissues. **(C)** Venn diagram showing the distribution of TFEB- $ERR\alpha$ axis related lipids and $ERR\alpha$ -dependent lipids in clinical samples. **(D)** Systematic lipidomic changes between EC and control tissues assessed by OPLS-DA. **(E)** Systematic lipidomic changes between LNM and non-LNM tissues assessed by OPLS-DA. **(F)** Significant lipid species in EC and normal control tissues and its PC/SM evaluation. **(G)** Analysis of TFEB- $ERR\alpha$ associated lipids, $ERR\alpha$ -dependent lipids and EC as well as LNM. **(H)** The univariate binary logistic regression analyses of Age, BMI, CA125, PC (18:1/18:2)+HCOO and PC (32:2)+H. **(I)** The correlation analysis of PC (18:1/18:2)+HCOO and $ERR\alpha$. *, $p < 0.05$. Statistical tests: Student's *t*-test(E-F), Logistic regression(G), Pearson's rank correlation analysis(H). BMI: Body Mass Index.

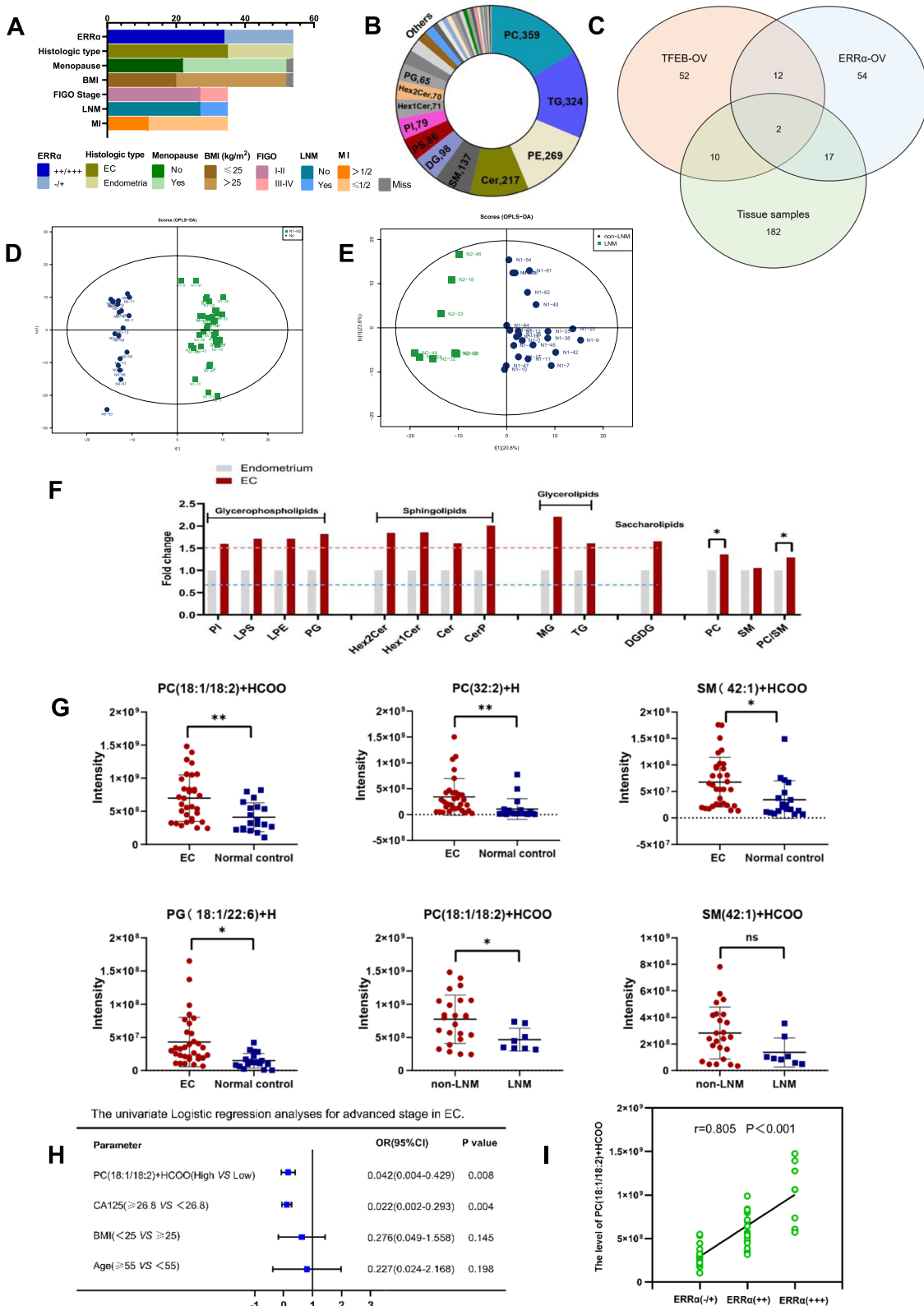


Fig. 7 (See legend on previous page.)

Table 2 Associations of PC(18:1/18:2)+HCOO with serum lipid

| Parameter | PC(18:1/18:2)+HCOO<cut-off value (n=23) | PC(18:1/18:2)+HCOO≥cut-off value (n=28) | p |
|---------------------|--|--|--------------|
| TG(mmol/L) | 1.533±0.650 | 2.911±9.981 | 0.136 |
| CHOL(mmol/L) | 5.379±1.062 | 5.329±1.258 | 0.904 |
| HDL (mmol/L) | 1.416±0.345 | 1.190±0.313 | 0.028 |
| APO-A(g/L) | 1.083±0.130 | 1.057±0.182 | 0.645 |
| LDL(mmol/L) | 3.367±0.958 | 2.960±0.757 | 0.221 |
| APO-B(g/L) | 1.011±0.261 | 0.961±0.200 | 0.573 |

Abbreviations: APO-A Apolipoprotein A, APO-B Apolipoprotein B, CHOL Cholesterol, HDL High-Density Lipoprotein, LDL Low-Density Lipoprotein, PC Phosphatidylcholine, TG total Triglyceride, Cut-off value=521540036.5. p < 0.05 suggests significantly different

In addition, increased PC (18:1/18:2) + HCOO has been shown to be a good predictor for prostate cancer [40]. In line with these findings, we found that PC (18:1/18:2) + HCOO was not only related to EC but also associated with EC metastasis, which showed a potential role of a tumor marker.

In summary, we found that the TFEB-ERR α signaling pathway regulates the invasion and metastasis of endometrial cancer cells through the EMT pathway and cell membrane fluidity. This regulation depends on ERR α to participate in the metabolism of lipids and cellular membrane remodeling. TFEB-ERR α enhances UFA-PCs, PG (18:1/22:6) + H and PC/SM in EC patients to promote cellular fluidity and results in invasion and metastasis. Furthermore, PC (18:1/18:2) + HCOO is the ERR α -dependent potential lipid to mediate EC metastasis. This also explains why ERR α , as a key factor in energy metabolism, is a poor prognostic factor for EC.

Abbreviations

ACADM: Medium-chain Acyl-coenzyme A Dehydrogenase; ACC: Acetyl-Co A Carboxylase; APO-A: Apolipoprotein A; ATCC: American Type Culture Collection; ATP: Adenosine Triphosphate; BMI: Body Mass Index; Cer: Ceramide; CerP: Ceramides Phosphate; ChIP-qPCR: Chromatin Immunoprecipitation Quantitative Polymerase Chain Reaction; CHOL: Cholesterol; CL: Cardiolipin; CNV: Copy Number Variation; DAVID: The Database for Annotation, Visualization and Integrated Discovery; DGDG: Digalactosyldiacylglycerol; DMEM: Dulbecco's Modification of Eagle's Medium Dulbecco; DMSO: Dimethyl Sulfoxide; EC: Endometrial Cancer; EEC: Endometrioid Endometrial Cancer; EMT: Epithelial-Mesenchymal Transformation; ER α : Estrogen receptor α ; ERR α /NR3B1/ESRRA: Estrogen-Related Receptor α ; FASN: Fatty Acid Synthase; FBS: Fetal Bovine Serum; FC: Fold Change; FCCP: Carbonyl cyanide 4-(trifluoromethoxy)phenylhydrazone; FIGO: Federation International of Gynecology and Obstetrics; GL: Glycerolipid; GM2: Gangliosides2; GP: Glycerophospholipid; GSEA: Gene Set Enrichment Analysis; HDL: High-Density Lipoprotein; HPLC: High Pressure Liquid Chromatography; IHC: Immunohistochemistry; IRS: Immunoreactive Score; KEGG: Kyoto Encyclopedia of Genes and Genomes; LC/MS: Liquid Chromatography Mass Spectrometry; LDL: Low-Density Lipoprotein; LNM: Lymph Node Metastasis; LPCAT: Lysophosphatidylcholine Acyltransferase; LPS: Lysophosphatidylserine; LPE: Lysophosphatidylethanolamine; MG: Monoglyceride; MI: Myometrial Invasion; MMP2: Matrix Metalloproteinase 2; NEEC: Non-Endometrioid Endometrial Cancer; OCR: Oxygen consumption rate; OPLS-DA: Orthogonal Partial Least Squares-Discriminant Analysis; OS: Overall Survival; PBS: Phosphate Buffered Solution; PC: Phosphatidylcholine; PE: Phosphatidylethanolamine; PG: Phosphatidylglycerol; PI: Phosphatidylinositol; PGC-1 α :

Peroxisome Proliferator-Activated Receptor Coactivator-1 α ; PPAR: Peroxisome Proliferator-Activated Receptor; PS: Phosphatidylserine; RT-qPCR: Reverse Transcription quantitative Polymerase Chain Reaction; ROC: Receiver Operating Characteristic; SFA: Saturated Fatty Acid; siRNA: Small Interfering RNA; SLs: Sphingolipids; SM: Sphingomyelin; SEM: Scanning Electron Microscope; TAG: Triacylglycerol; TCGA: The Cancer Genome Atlas; TFEB: Transcription Factor EB; TG: total Triglyceride; TMA: Tissue Microarray; TMT: Tandem Mass Tags; UCEC: Uterine Corpus Endometrial Carcinoma; UCSC: University of California, Santa Cruz; UFA: Unsaturated Fatty Acid; WB: Western Blotting.

Supplementary Information

The online version contains supplementary material available at <https://doi.org/10.1186/s13046-021-02211-2>.

Additional file 1: **Figure S1.** The flow chart of study participants. Abbreviation: APO-A, a polipoprotein A; APO-B, a polipoprotein B; BMI, Body Mass Index; CA125, Cancer antigen 125; CHOL, Cholesterol; Con, Control; EC, Endometrial cancer; ERR α , Estrogen-Related Receptor α ; FIGO, Federation International of Gynecology and Obstetrics; HDL, High-Density Lipoprotein; IHC, Immunohistochemistry; IRS, Immunoreactive Score; LDL, Low-Density Lipoprotein; LNM, Lymph Node Metastasis; LC/MS, Liquid Chromatography Mass Spectrometry; PC, Phosphatidylcholine; PE, Phosphatidylethanolamine; TAG, Triacylglycerol; TG, Total Triglyceride; TFEB, transcription factor EB. **Figure S2.** The ROC curve of PC (18:1/18:2) + HCOO, PC (32:2) + H, HDL and CA125. **Figure S3.** Hypothesis diagram of lipid reprogramming in EC cells modulated by TFEB-ERR α axis. **Table S1.** The overlapped lipids between TFEB and ERR α over-expressing. **Table S2.** Significant proteins derived from omics analysis.

Acknowledgements

Thanks are due to Central Laboratory, Fujian Medical University Union Hospital for assistance with the experiments and to Zhenli Li, Lili Chen, Meimei Huang and Tingting Jiang for their assistance with the methods and literature retrieval.

Authors' contributions

XiaoDan Mao designed the experiments and wrote the paper. Huifang Lei, Tianjin Yi conducted the partial experiments, data analysis and fund support. Pingping Su and ShuTing Tang conducted the experiments and contributed to the analysis of data. Binhua Dong and Guanyu Ruan contributed to the methods and performed the laboratory analyses, and provided valuable discussion. Alexander Mustea and Jalid Sehouli contributed to critically revised the article for important intellectual content. PengMing Sun contributed to the acquisition of data, critically revised the article for important intellectual content, and supervised the study. All authors gave their final approval of the version to be submitted.

Funding

This work was supported by grants from the Fujian Provincial Nature Science Foundation of China (Grant no. 2017Y9062, 2017J01233, 2020J02059,

2021J01404), Joint Funds for the Innovation of Science and Technology, Fujian Province (Grant no. 2020Y9160) and National Nature Science Foundation of China (Grant no.82002756).

Availability of data and materials

The datasets analyzed during the current study are available from the corresponding author on reasonable request.

Declarations

Ethics approval and consent to participate

This research protocol was approved by the Ethics Committee of Fujian Provincial Maternity and Child Health Hospital, Affiliated Hospital of Fujian Medical University (No. FMCH-2018–14).

Consent for publication

Not applicable.

Competing interests

The authors declare that they have no competing interests.

Author details

¹Laboratory of Gynecologic Oncology, Department of Gynecology, Fujian Maternity and Child Health Hospital, Affiliated Hospital of Fujian Medical University, No. 18 Daoshan Road, Fuzhou 350001, China. ²School of Medical Technology and Engineering, Fujian Medical University, No.88 Jiaotong Road, Fuzhou 350004, China. ³Fujian Key Laboratory of Women and Children's Critical Diseases Research, No. 18 Daoshan Road, Fuzhou 350001, China. ⁴National Health Commission Key Laboratory of Technical Evaluation of Fertility Regulation for Non-Human Primate, Jinjishan Road 19, Fuzhou 350005, China. ⁵Department of Obstetrics and Gynecology, Key Laboratory of Birth Defects and Related Diseases of Women and Children of MOE and State Key Laboratory of Biotherapy, West China Second University Hospital, Sichuan University and Collaborative Innovation Center, Chengdu 610041, China. ⁶Department of Gynecology and Gynecological Oncology, University Hospital Bonn, Venusberg-Campus 1, 53127 Bonn, Germany. ⁷Department of Gynecology and Obstetrics, Charité Virchow University Hospital, Augustenberger Platz 1, 13353 Berlin, Germany.

Received: 7 September 2021 Accepted: 4 December 2021

Published online: 19 January 2022

References

1. Swinburn BA, et al. The Global Syndemic of Obesity, Undernutrition, and Climate Change: The Lancet Commission report. *Lancet*. 2019;393:791–846.
2. Sung H, et al. Global patterns in excess body weight and the associated cancer burden. *CA Cancer J Clin*. 2019;69:88–112.
3. Siegel RL, Miller KD, Fuchs HE, Jemal A. Cancer Statistics, 2021. *CA Cancer J Clin*. 2021;71:7–33.
4. Chen W, et al. Cancer statistics in China, 2015. *CA Cancer J Clin*. 2016;66:115–32.
5. Giguère V, Yang N, Segui P, Evans RM. Identification of a new class of steroid hormone receptors. *Nature*. 1988;331:91–4.
6. Deblois G, St-Pierre J, Giguère V. The PGC-1/ERR signaling axis in cancer. *Oncogene*. 2013;32:3483–90.
7. De Vitto H, et al. Estrogen-related receptor alpha directly binds to p53 and cooperatively controls colon cancer growth through the regulation of mitochondrial biogenesis and function. *Cancer Metab*. 2020;8:28.
8. Deblois G, Giguère V. Oestrogen-related receptors in breast cancer: control of cellular metabolism and beyond. *Nat Rev Cancer*. 2013;13:27–36.
9. Valcarcel-Jimenez L, et al. PGC1 α Suppresses Prostate Cancer Cell Invasion through ERR α Transcriptional Control. *Cancer Res*. 2019;79:6153–65.
10. Sun P, et al. Expression of estrogen receptor-related receptors, a subfamily of orphan nuclear receptors, as new tumor biomarkers in ovarian cancer cells. *J Mol Med (Berl)*. 2005;83:457–67.
11. Chen L, et al. PGC-1 α and ERR α in patients with endometrial cancer: a translational study for predicting myometrial invasion. *Aging (Albany NY)*. 2020;12:16963–80.
12. Sun P, et al. Novel endocrine therapeutic strategy in endometrial carcinoma targeting estrogen-related receptor α by XCT790 and siRNA. *Cancer Manag Res*. 2018;10:2521–35.
13. Zhitomirsky B, Assaraf YG. Lysosomes as mediators of drug resistance in cancer. *Drug Resist Updat*. 2016;24:23–33.
14. Settembre C, et al. TFEB controls cellular lipid metabolism through a starvation-induced autoregulatory loop. *Nat Cell Biol*. 2013;15:647–58.
15. Wu Y, et al. Phospholipid remodeling is critical for stem cell pluripotency by facilitating mesenchymal-to-epithelial transition. *Sci Adv*. 2019;5:eaaax7525.
16. Wang B, Tontonoz P. Phospholipid Remodeling in Physiology and Disease. *Annu Rev Physiol*. 2019;81:165–88.
17. van Meer G, Voelker DR, Feigenson GW. Membrane lipids: where they are and how they behave. *Nat Rev Mol Cell Biol*. 2008;9:112–24.
18. Bi J, et al. Oncogene Amplification in Growth Factor Signaling Pathways Renders Cancers Dependent on Membrane Lipid Remodeling. *Cell Metab*. 2019;30:525–538.e528.
19. Lin L, et al. Functional lipidomics: Palmitic acid impairs hepatocellular carcinoma development by modulating membrane fluidity and glucose metabolism. *Hepatology*. 2017;66:432–48.
20. Wang C, et al. Hepatocellular Carcinoma-Associated Protein TD26 Interacts and Enhances Sterol Regulatory Element-Binding Protein 1 Activity to Promote Tumor Cell Proliferation and Growth. *Hepatology*. 2018;68:1833–50.
21. Smith DC, Prentice R, Thompson DJ, Herrmann WL. Association of exogenous estrogen and endometrial carcinoma. *N Engl J Med*. 1975;293:1164–7.
22. Guo H, et al. Reversal of obesity-driven aggressiveness of endometrial cancer by metformin. *Am J Cancer Res*. 2019;9:2170–93.
23. Deblois G, et al. ERR α mediates metabolic adaptations driving lapatinib resistance in breast cancer. *Nat Commun*. 2016;7:12156.
24. Wallace M, Metallo CM. PGC1 α drives a metabolic block on prostate cancer progression. *Nat Cell Biol*. 2016;18:589–90.
25. Mao X, et al. Dual targeting of estrogen receptor α and estrogen-related receptor α : a novel endocrine therapy for endometrial cancer. *Onco Targets Ther*. 2019;12:6757–67.
26. You Y, et al. Sorting Nexin 10 Mediates Metabolic Reprogramming of Macrophages in Atherosclerosis Through the Lyn-Dependent TFEB Signaling Pathway. *Circ Res*. 2020;127:534–49.
27. Zhang Z, et al. The unfolded protein response regulates hepatic autophagy by sXBP1-mediated activation of TFEB. *Autophagy*. 2020;1:15.
28. Zhang C, et al. TFEB mediates immune evasion and resistance to mTOR inhibition of renal cell carcinoma via induction of PD-L1. *Clin Cancer Res*. 2019;25:6827–38.
29. Martini-Stoica H, Xu Y, Ballabio A, Zheng H. The Autophagy-Lysosomal Pathway in Neurodegeneration: A TFEB Perspective. *Trends Neurosci*. 2016;39:221–34.
30. Evans T. D, et al. TFEB drives PGC-1 α expression in adipocytes to protect against diet-induced metabolic dysfunction. *Sci Signal*. 2019;12:eaaau2281.
31. A. Jonas, M.C. Phillips, Lipoprotein structure, in: D.E. Vance, J.E. Vance (Eds.), *Biochemistry of Lipids, Lipoproteins and Membranes*, 5th Edition, Elsevier, sterdam, 2008, pp. 485–506.
32. Swinnen JV, Dehairs J, Talebi A. Membrane Lipid Remodeling Takes Center Stage in Growth Factor Receptor-Driven Cancer Development. *Cell Metab*. 2019;30:407–8.
33. Wang B, et al. Phospholipid Remodeling and Cholesterol Availability Regulate Intestinal Stemness and Tumorigenesis. *Cell Stem Cell*. 2018;22:206–220.e204.
34. Plumb JA, Luo W, Kerr DJ. Effect of polyunsaturated fatty acids on the drug sensitivity of human tumour cell lines resistant to either cisplatin or doxorubicin. *Br J Cancer*. 1993;67(4):728–33.
35. Flis V. V, Daum G. Lipid transport between the endoplasmic reticulum and mitochondria. *Cold Spring Harb Perspect Biol*. 2013;5(6):a013235.
36. Zinser E, et al. Phospholipid synthesis and lipid composition of subsellular membranes in the unicellular eukaryote *Saccharomyces cerevisiae*. *J Bacteriol*. 1991;173:2026–34.

37. Gouw AM, et al. The MYC Oncogene Cooperates with Sterol-Regulated Element-Binding Protein to Regulate Lipogenesis Essential for Neoplastic Growth. *Cell Metab.* 2019;30:556–572.e555.
38. Mühleip A, et al. ATP synthase hexamer assemblies shape cristae of *Toxoplasma* mitochondria. *Nat Commun.* 2021;12(1):120.
39. Friedman JR, et al. Lipid Homeostasis Is Maintained by Dual Targeting of the Mitochondrial PE Biosynthesis Enzyme to the ER. *Dev Cell.* 2018;44:261–270.e266.
40. Forajta M B, et al. Lipidomics as a Diagnostic Tool for Prostate Cancer. *Cancers (Basel).* 2021;13:2000.

Publisher's Note

Springer Nature remains neutral with regard to jurisdictional claims in published maps and institutional affiliations.

Ready to submit your research? Choose BMC and benefit from:

- fast, convenient online submission
- thorough peer review by experienced researchers in your field
- rapid publication on acceptance
- support for research data, including large and complex data types
- gold Open Access which fosters wider collaboration and increased citations
- maximum visibility for your research: over 100M website views per year

At BMC, research is always in progress.

Learn more biomedcentral.com/submissions

